Simulation of Phytoremediation of a TNT-Contaminated Soil Using the CTSPAC Model

Y. Ouyang,* D. Shinde, and L. Q. Ma

ABSTRACT

Knowledge of water movement in the plant-xylem system and contaminant bioavailability in the soil environment is crucial to evaluate the success of phytoremediation practices. This study investigated the removal of 2,4,6-trinitrotoluene (TNT) from a contaminated sandy soil by a single poplar (*Populus fastigiata*) tree through the examinations of temporal variations of xylem water potential, root water uptake, and soil TNT bioavailability. A mathematical model, CTSPAC (Coupled Transport of water, heat, and solutes in the Soil–Plant–Atmosphere Continuum), was modified for the purpose of this study. The model was calibrated using laboratory measurements before its application. Our simulations show that the xylem water potential was high in the roots and low in the leaves with a potential head difference of 3.55 cm H_2O, which created a driving force for water flow and chemical transport upward from the roots through the stem to the leaves. The daily average root water uptake rate was 25 cm^3 h^{-1} when an equilibrium condition was reached after 24 h. Our simulations further reveal that no TNT was found in the stem and leaves and only about 1% of total TNT mass was observed in the roots due to the rapid biodegradation and transformation of TNT into its daughter products. About 13% of the soil TNT was removed by the poplar tree, resulting mainly from root uptake since TNT is a recalcitrant compound. In general, the soil TNT bioavailability decreased with time due to the depletion of soil solution TNT by the poplar tree. A constant bioavailability (i.e., 3.1×10^{-6}) was obtained in 14 d in which the soil TNT concentration was about 10 mg L^{-1}. Our study suggests that CTSPAC is a useful model to simulate phytoremediation of TNT-contaminated sites.

ORGANIC CONTAMINANTS are ubiquitous in soil and ground water systems throughout the world. Most of these contaminants are hydrophobic and persistent in the environment. One such organic contaminant is TNT, which was introduced into soil and ground water mainly through improper explosive manufacturing, storage, testing, and packaging. As a result, thousands of acres of soil contaminated with TNT need to be remediated (Voudrias and Assaf, 1996). Incineration, compost application, and oxygen releasing compounds (ORC) are currently available technologies for remediation of highly toxic soils contaminated with TNT. Incineration is the preferred technology for remediation of munitions-contaminated soil, but is hindered by energy cost, corrosion problems, and the ecological process that can disseminate dust into the atmosphere (Arienzo, 2000). Compost application is an economical method for remediating explosive-contaminated soils and has been found to reduce the concentrations of target contaminants such as TNT. However, the potential for ecotoxicological effects of unknown products remains because the mutagenicity of the soil is markedly increased during compost application (Jarvis et al., 1998). In recent years there has been a growing interest toward the use of ORC, such as sodium percarbonate and metal peroxides. The ORC technology is being used on more than 2000 sites in 46 states of the United States and several other countries. This technology is intended to promote direct oxidation of contaminants and enhance in situ aerobic microbial degradation (Arienzo, 2000).

Phytoremediation is the use of plants to remediate selected contaminants in contaminated soil, sludge, sediment, ground water, surface water, and waste water. It utilizes a variety of plant-based biological processes and the physical characteristics of plants to aid in situ remediation (Pivetz, 2001; Trapp and Karlson, 2001). Uptake of TNT by plants has been studied during the past decade (Kaplan, 1990; Schackmann, and Muller, 1991; Schnoor et al., 1995; Voudrias and Assaf, 1996; Hughes et al., 1997). These studies were initially prompted by a concern over effects on the food chain of plants exposed to TNT contamination and are recently driven by interests in phytoremediation.

Mueller et al. (1995) studied the uptake and biotransformation of TNT in cell suspension cultures and in whole plants of Jimson weed (*Datura innoxia* Mill.) and tomato [*Lycopersicon peruvianum* (L.) Mill.]. In cell culture, TNT was rapidly removed from the growth medium and recovered from the cell extract in the form of a variety of biotransformation products resulting from nitroreduction, deamination, N-acetylation, and side chain oxidation to aldehyde and carboxylic acid metabolites. Whole plants of the same species grew well in soils contaminated with TNT up to 750 μg g^{-1}, but showed some signs of phytotoxicity for the *Datura* plants and a severe effect on the *Lycopersicon* plants at 1000 μg g^{-1}. Both species removed TNT from soil and stored its metabolites at levels up to 30 times higher than the soil TNT concentrations. After a two-week growth period, only 4 to 9.2% of the applied TNT was found in the soils. Thompson et al. (1998) showed that TNT was strongly bonded and transformed by the root tissues, and it only translocated slightly to the leaves of the poplar cuttings. TNT was transformed by the poplar trees to its daughter products such as 4-amino-2,6-dinitrotoluene, 2-amino-

---

Y. Ouyang, Department of Water Resources, St. Johns River Water Management District, P.O. Box 1429, Palatka, FL 32178-1429. D. Shinde and L.Q. Ma, Soil and Water Science Department, University of Florida, Gainesville, FL 32611-0290. Approved for publication as Florida Agricultural Experiment Station Journal Series no. R-10827. Received 13 December 2004. *Corresponding author (youyang@sjrwmd.com).

Published in J. Environ. Qual. 34:1490–1496 (2005).
Technical Reports: Bioremediation and Biodegradation
doi:10.2134/jeq2004.0471

677 S. Segoe Rd., Madison, WI 53711 USA

Abbreviations: CTSPAC, Coupled Transport of water, heat, and solutes in the Soil–Plant–Atmosphere Continuum; TNT, 2,4,6-trinitrotoluene.

4,6-dinitrotoluene, and a number of unidentified compounds. Recently, Chang et al. (2004) demonstrated that Indian mallow [*Abutilon avicennae* (P.) Mill.] enhanced TNT removal and retarded TNT migration in soil by stimulating microbial TNT transformation and by facilitating direct uptake and phytotransformation of TNT.

Although phytoremediation technology has shown significant potential for removal of contaminants from surface and subsurface environments (Schnoor et al., 1995; Mueller et al., 1995; Pivetz, 2001; Thompson et al., 1998; Aitchison et al., 2000; Nedunuri et al., 2000; Chang et al., 2004), the effects of plant physiological, microbiological, and hydrological conditions on its applications are still poorly understood. A thorough literature search reveals that insufficient research effort has been devoted to developing mathematical models for a comprehensive investigation of phytoremediation of contaminants in the soil–plant–air system.

Recently, Ouyang (2002) modified the CTSPAC model to simulate phytoremediation of dioxane by the poplar cuttings in the soil–plant–atmosphere continuum. This one-dimensional mathematical model was originally developed for the vadose zone as controlled by atmospheric, soil physical, and biological conditions (Lindstrom et al., 1990; Boersma et al., 1991). The feasibility of the modified CTSPAC model to predict the uptake and accumulation of dioxane by poplar cuttings was tested against the laboratory measurements before its applications. A simulation scenario was then performed to investigate phytoremediation of dioxane by poplar cuttings associated with daily water flow and dioxane transport, uptake, and accumulation in the soil and poplar cuttings for a simulation period of 7 d. Ouyang (2002) found that dioxane concentration was high in the leaf compartments and low in the root compartments with the stem compartments in between. Although the study provided insight into the phytoremediation of dioxane in the soil–plant–atmosphere continuum, no effort has been devoted to investigating the phytoremediation of soil contaminated with TNT in response to the xylem water flow and soil TNT bioavailability.

The primary purpose of this study was to investigate the removal of TNT from a contaminated sandy soil by a poplar tree through the simulations of temporal variations of xylem water potential, root water uptake, and soil TNT bioavailability. The specific objectives were to (i) calibrate the CTSPAC model for simulating phytoremediation of TNT using the laboratory experimental data reported by Thompson et al. (1998); (ii) investigate the temporal variations of xylem water potential, and root water and TNT uptake; and (iii) examine soil TNT bioavailability and removal from a contaminated soil. The poplar tree was selected in this study partially because of its high TNT uptake capacity and partially because of the availability of experimental data (Thompson et al., 1998) for model calibrations.

MATERIALS AND METHODS

Model Description

The CTSPAC model consists of coupling a soil submodel to a plant submodel (Lindstrom et al., 1990; Boersma et al., 1991). The soil submodel has three time-dependent governing equations for vertical simultaneous flow and transport of water, solutes, and heat through the vadose zone. Water movement is modeled using the Richards equation associated with the effects of daily cycles of surface water infiltration and evaporation, root water uptake, and leaf transpiration. Soil heat flux is described by heat conduction in the solid, liquid, and air phases; by heat convection in the liquid phase; and by the transport of latent heat. Chemical transport is described by the mechanisms of convection, dispersion–diffusion, sorption, degradation, and root uptake. The equation for water movement through the vadose zone used by the soil submodel is:

$$V_{\mathrm{REV_s}}\left\{\frac{\partial(\rho_{\mathrm{w}}\theta)}{\partial t}+\frac{\partial(\rho_{\mathrm{w}}\theta V_{\mathrm{l}})}{\partial z}+\frac{\partial[\rho_{\mathrm{wv}}(\varepsilon-\theta)V_{\mathrm{wv}}]}{\partial z}\right\} = q_{\mathrm{w_s}}(z,t)A_{\mathrm{PR}}(z) \qquad [1]$$

where $V_{\mathrm{REV_s}}$ is the representative elementary soil volume (cm^3); ρ_{w} and ρ_{wv} the densities of water and water vapor (g cm^3), respectively; θ the volumetric water content (cm^3 cm^{-3}); t the time (h); V_{l} and V_{wv} the velocities of liquid and vapor phase water (cm h^{-1}), respectively; z the soil depth (cm); ε the soil porosity (cm^3 cm^{-3}); $q_{\mathrm{w_s}}(z,t)$ the water flux due to root extraction (g cm^{-2} h^{-1}); and $A_{\mathrm{PR}}(z)$ the effective soil–root contact area (cm^2).

The equation for heat flux through the unsaturated soil is:

$$V_{\mathrm{REV_s}}\left\{\frac{\partial}{\partial t}[(1-\varepsilon)C_{\mathrm{solid}}\rho_{\mathrm{solid}}T + (\varepsilon-\theta)C_{\mathrm{air}}\rho_{\mathrm{air}}T + \theta C_{\mathrm{w}}\rho_{\mathrm{w}}T] + \frac{\partial}{\partial z}[(1-\varepsilon)H_{\mathrm{ss}} + \theta H_{\mathrm{sl}} + (\varepsilon-\theta)H_{\mathrm{sv}}]\right\} = A_{\mathrm{PR}}q_{\mathrm{w_s}}(z)C_{\mathrm{w}}T \qquad [2]$$

where C_{solid} is the specific heat of soil particles (J cm^{-1} h^{-1} K^{-1}); ρ_{solid} and ρ_{air} the densities of soil particles and air (g cm^{-3}), respectively; C_{air} and C_{w} the specific heats of air and water (J cm^{-1} h^{-1} K^{-1}), respectively; H_{ss} the heat conduction through soil particles (J cm^{-2} h^{-1}); H_{sl} the heat conduction and convection in the liquid phase (J cm^{-2} h^{-1}); and H_{sv} the heat conduction in the vapor phase and the transport of latent heat (J cm^{-2} h^{-1}).

The equation for solute transport and fate is:

$$V_{\mathrm{REV_s}}\left\{\frac{\partial}{\partial t}[\theta + (\varepsilon-\theta)H_{\mathrm{c}})C_{\mathrm{l}} + (1-\varepsilon)S] + [\theta + (\varepsilon-\theta)H_{\mathrm{c}}]\Lambda C_{\mathrm{l}} + \frac{\partial}{\partial z}[\theta q_{\mathrm{cl}} + (\varepsilon-\theta)q_{\mathrm{cv}}]\right\} = \begin{cases} A_{\mathrm{PR}}(z)q_{\mathrm{w_s}}(z,t)C_{\mathrm{l}}(z,t) & \mathit{for}\ q_{\mathrm{w}} \le 0 \\ A_{\mathrm{PR}}(z)q_{\mathrm{w_s}}(z,t)C_{\mathrm{PR}}(z,t) & \mathit{for}\ q_{\mathrm{w}} > 0 \end{cases} + A_{\mathrm{PR}}q_{\mathrm{rs}} + V_{\mathrm{REV_s}}Q_{\mathrm{so}}(z,t) \qquad [3]$$

where C_{l} is the concentration of solute in the liquid phase (μg cm^{-3}); H_{c} the Henry's law constant (cm^3 cm^{-3}); S the average concentration of solute in the sorbed phase; Λ the cumulative first-order loss coefficient (h^{-1}); q_{cl} and q_{cv} the solute fluxes in the liquid and vapor phases (μg cm^{-3} h^{-1}), respectively; C_{PR} the solute concentration inside the plant root (μg cm^{-3}); q_{rt} the solute diffusive flux through the soil near the root–soil interface (μg cm^{-2} h^{-1}); and Q_{so} the sources of solute (μg cm^{-3} h^{-1}).

In CTSPAC, compartmentalization of a plant into local regions of similar tissue structure and function is used. Compartments are chosen to account for important flow processes, including (i) water uptake by roots; (ii) water transport driven by gradients of total water potential through roots, stems, and leaves in both xylem and phloem; (iii) chemical transport in phloem driven by a gradient of positive pressure; and (iv) water vapor flow from intercellular spaces to the atmosphere for evapotranspiration, and control of water vapor loss and carbon dioxide uptake through stomata. Figure 1 shows the compartments for roots, stems, and leaves of a generic plant. These compartments contain the actual physiological and anatomical structures and functions of xylem and phloem. Each compartment should be visualized as a transport unit. Water moves from the soil to the atmosphere through the compartments. Leaves are represented by individual xylem and phloem parts, which contain the mesophyll, intercellular air space, stomatal cavities, and stomatal pore regions. Water also moves from xylem to phloem compartments and vice versa in roots, stems as well as in leaves. This movement is driven by water potential gradients that are affected by the sugar concentrations in these compartments. As sugar accumulates in the leaf, the total water potential decreases and water flows from xylem to phloem. In the root, water flows from phloem to xylem when sugar is unloaded and stored (Nobel, 1983). Transport in the phloem is modeled as pressure-driven flow according to the Münch hypothesis.

The equation for water movement in plant tissues between compartments is:

$$Q^{ij} = -A^{ij}L^{ij}(\psi_t^j - \psi_t^i)(\tilde{K}) \qquad [4]$$

where Q^{ij} is the volume flow rate (cm^3 h^{-1}) between adjacent compartments i and j, L^{ij} the conductance (cm h^{-1} MPa^{-1}) between compartments i and j, and $\tilde{K}$ the unit vector for positive vertical flow direction downward (dimensionless).

Based on radioisotope technique, it has been shown that little TNT was translocated into the aboveground parts of plant species and TNT in plant tissues was present in the form of more polar metabolites (Mueller et al., 1995; Thompson et al., 1998). To simulate the translocation of TNT metabolites rather than TNT itself in the plant compartments, the existing CTSPAC model is modified with the assumption that once in contact with the root surface or across the root membrane

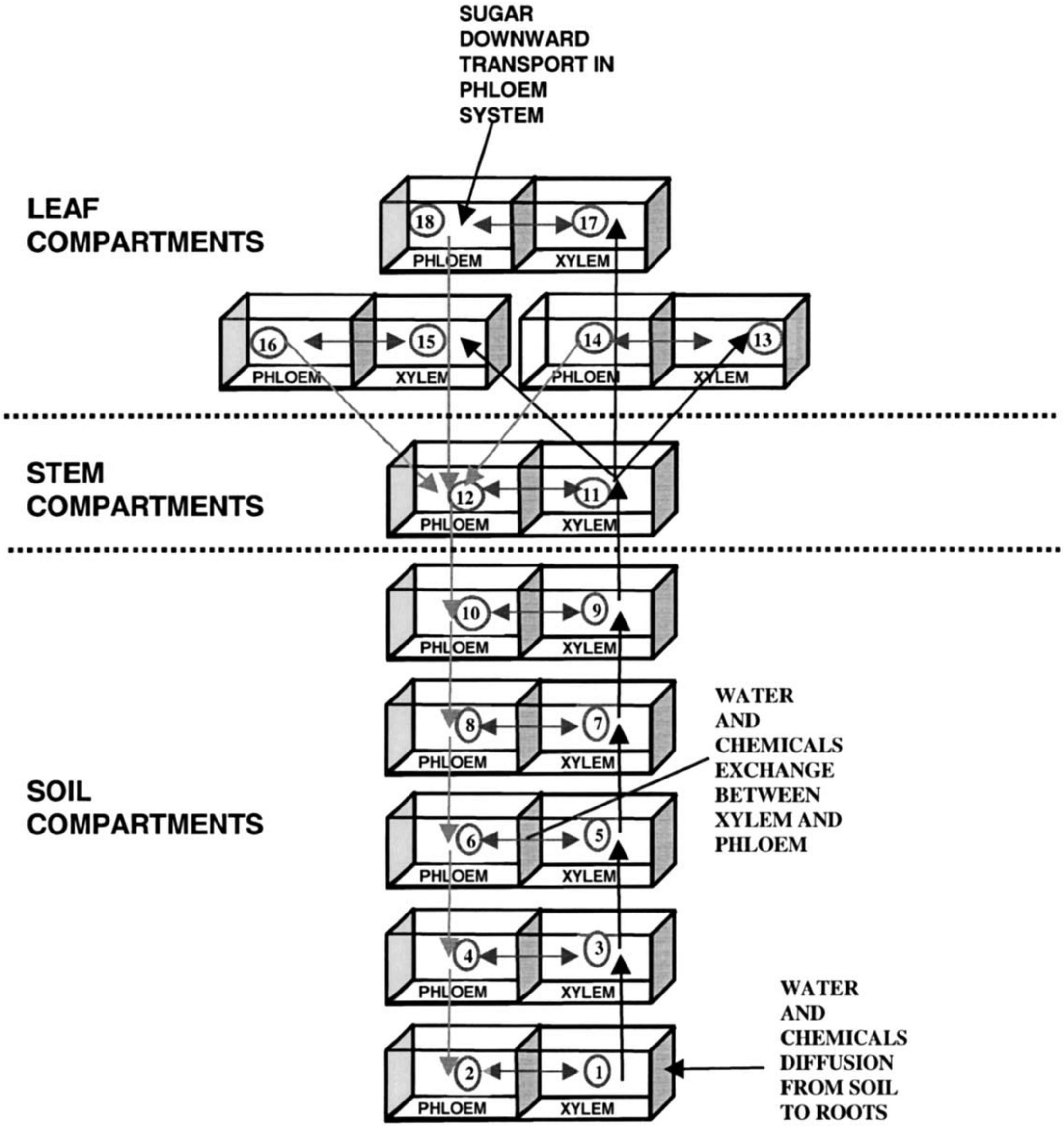

Fig. 1. Schematic diagram showing a compartment model for chemical transport within a plant system. The numbers are the plant compartment numbers.

from the soil–root interface, TNT is degraded into its metabolites.

The equations, developed by Lindstrom et al. (1990), for the transport and storage of a solute in compartments are modified for TNT metabolites in this study. For example, the transport and storage of the TNT metabolites in Compartment 1 (Fig. 1) can be written as:

$$\frac{\mathrm{d}M_{\mathrm{P1}}}{\mathrm{d}t} = \left[\frac{D_{\mathrm{c}}}{\Delta x_{\mathrm{mb}}} A_1(C_1^{\mathrm{P}} - C_{\mathrm{P1}}) - Q_1(1 - \sigma_1)C_1^{\mathrm{P}}\right] - \left[\frac{D_2}{\Delta x_2} A_2(C_{\mathrm{P1}} - C_{\mathrm{P3}}) - |Q_2|(1 - \sigma_2)C_{\mathrm{P1}}\right] + \left[\frac{D_4}{\Delta x_4} A_4(C_{\mathrm{P2}} - C_{\mathrm{P1}}) - |Q_4|(1 - \sigma_4)C_{\mathrm{P2}}\right] - S_1^{\mathrm{Stor}} C_{\mathrm{P1}} - \lambda_1 M_1 \qquad [5]$$

where M_{P1} is the mass of TNT metabolites in Compartment 1 (μg), D_{c} the effective diffusivity of TNT metabolites cross the root membrane into the root interior (cm^2 h^{-1}), Δx_{mb} the thickness of root membrane (cm), A_1 the contact area between soil and Compartment 1(cm^2), A_2 the contact area between Compartment 1 and Compartment 2 in the xylem system (cm^2), A_4 the contact area between Compartment 1 in the xylem system and Compartment 1 in the phloem system (cm^2), C_1^{P} the concentration of TNT metabolites resulting from TNT degradation at the surface of root membrane or at the very moment of entering the membrane (μg cm^{-3}), C_{P1} the concentration of TNT metabolites in Compartment 1 in the xylem system (μg cm^{-3}), Q_1 the water flow rate from soil into roots in Compartment 1 in the xylem system (cm^3 h^{-1}), Q_2 the water flow rates between Compartment 1 and Compartment 2 in the xylem system (cm^3 h^{-1}), Q_4 the water flow rates between Compartment 1 in the xylem system and Compartment 1 in the phloem system (cm^3 h^{-1}), σ_1 the reflection coefficient of TNT metabolites from soil into roots in Compartment 1 in the xylem system (dimensionless), σ_2 the reflection coefficient of TNT metabolites between Compartment 1 and Compartment 2 in the xylem system (dimensionless), σ_4 the reflection coefficient of TNT metabolites between Compartment 1 in the xylem system and Compartment 1 in the phloem system (dimensionless), S_1^{Stor} the effective first-order TNT metabolites chemical storage rate in Compartment 1 (cm^3 h^{-1}), and λ_i the rate constant for all other first-order loss processes in Compartment 1 describing immobilization of TNT metabolites by incorporation into structural materials or loss of the metabolites due to metabolism (h^{-1}). Equations for the transport and storage of the TNT metabolites in other compartments can be postulated in a similar fashion.

The soil and plant submodels are both coupled to the atmospheric conditions, which are the highly nonlinear and dynamic top boundary conditions. These boundary conditions include daily cycles of soil temperature that are determined by the energy balance at the soil surface, daily cycles of leaf water transpiration and soil evaporation, daily variations of air temperature and relative humidity, and daily cycle of irrigation or rainfall event. A detailed description of the atmospheric conditions and the CTSPAC model can be found in Lindstrom et al. (1990) and Boersma et al. (1991).

Model Calibration

Before applying the CTSPAC model to simulate phytoremediation of TNT by poplar trees, the following three input parameter values must be known: (i) effective xenobiotic diffusivity of TNT at the soil–root interface; (ii) compartmental TNT reflections (i.e., the ease with which TNT crosses the membrane between the xylem and the phloem); and (iii) TNT storage rates in the plant compartments. The values of these parameters vary with each plant species. In this study, we attempted to obtain these values through model calibrations using the fresh soil data reported by Thompson et al. (1998). Thompson et al. (1998) studied the phytoremediation of TNT by hybrid poplar trees in both hydroponic and soil (fresh soil and aged soil) experiments. It was found that about 75% of the TNT remained in the soil in their fresh soil experiment. Of the 25% being taken up by the trees, no TNT was found in stems and leaves and only 0.35% in the roots. Results indicate that almost all of the TNT taken up by the trees was degraded and transformed into more polar products.

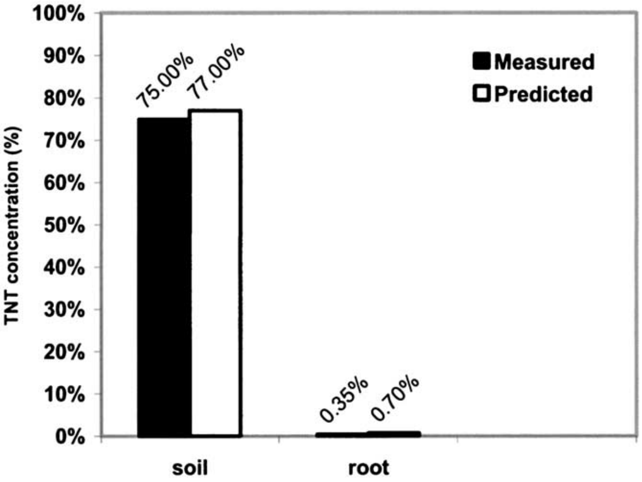

Fig. 2. Comparison of the predicted and the measured TNT concentrations in soil and roots during model calibration process.

Model calibrations were accomplished by adjusting the values of the three types of coefficients by trial and error until the model predictions matched the experimental measurements. Comparison of measured and predicted TNT concentrations in soil and roots for the fresh soil experiment is shown in Fig. 2. A good calibration was obtained between the model predictions and the experimental measurements. The calibrated values for the three parameters are given in Table 1. Notice that no literature values for those three calibrated parameters are available for comparisons in any phytoremediation of TNT study although these calibrated values are within the ranges reported by Boersma et al. (1988) who studied the uptake of organic chemicals by a soybean [*Glycine max* (L.) Merr.] plant.

Model Scenario

A simulation scenario was performed to investigate the phytoremediation of TNT for a simulation period of 30 d. A sandy soil containing 110 mg L^{-1} TNT with a depth of 100 cm and a poplar tree with a total volume of 30.8 cm^3 were selected as the modeled domain. The poplar tree was assumed to have an averaged root volume of 12.0 cm^3, which was equally divided into five sectors: a stem of 14.0 cm^3 as one sector, and three-leaf clusters with a total volume of 4.8 cm^3, which were equally divided into three sectors. Each sector was further divided into two compartments (one for xylem and the other for phloem), and thereby resulting in 18 plant compartments. The conceptual diagram of the plant compartment layout used in this study is the same as in Fig. 1. This poplar tree was estimated to have an aboveground height of 18.8 cm. Detailed description of the conceptual model showing plant compart-

Table 1. Values of input parameters used in this study.

Parameter	Value	Reference or remark
	Simulation controls	
Simulation time step, h	0.1	assumed
Simulation time period, h	72	assumed
Simulation soil depth, cm	100	assumed
Irrigation rate, mm h^{-1}	0.5	assumed
Irrigation duration, h d^{-1}	2.5	assumed
	Soil properties	
Soil type	sand	assumed
Soil porosity, cm^3 cm^{-3}	0.45	Hillel (1982)
Hydraulic conductivity, cm h^{-1}	0.1	Hillel (1982)
Initial soil water content, cm^3 cm^{-3}	0.3	assumed
Initial soil temperature, °C	20	assumed
Initial soil solution TNT concentration, μg cm^{-3}	110	assumed
Diffusion coefficient in the soil liquid phase, cm^2 h^{-1}	1.1×10^{-9}	Voudrias and Assaf (1996)
Effective soil–root interface membrane diffusivity, cm^2 h^{-1}	1.8×10^{-8}	Boersma et al. (1991), Ouyang (2002)
	Plant compartments	
Contact area between compartments, cm^2	ranging from 0 to 848	Boersma et al. (1991), Ouyang (2002)
Plant compartment water conductivity, cm h^{-1}	ranging from 0 to 10 000	Boersma et al. (1991), Ouyang (2002)
TNT reflection coefficients in compartments	0.65	calibrated
TNT sorption coefficient in compartments, h^{-1}	0.001	calibrated
Effective plant root xenobiotic diffusivity for TNT, cm^2 h^{-1}	1.8×10^{-8}	calibrated
Parameter for stomata control function	ranging from 1 to 20.7	Ouyang (2002)
Thickness of soil sheath around each rootlet, cm	0.2	Ouyang (2002)
Average diameter of rootlet, cm	0.0158	Ouyang (2002)
Number of rootlets	2769	Ouyang (2002)
	Atmospheric conditions	
Average air temperature, °C	25	assumed
Relative humidity	0.9	assumed
Average solar radiation, J cm^2 h^{-1}	59	assumed

ments along with a plant system can be found in Ouyang (2002). Table 1 lists the major input parameter values used this study.

RESULTS AND DISCUSSION

Xylem Water Potential

The xylem and phloem of a plant make up the vascular systems in the roots, stems, and leaves. In a tree trunk the phloem constitutes a layer of the bark, while the xylem constitutes almost all of the wood. The xylem commonly provides structural support for plants. The upward transport of water and chemical from soil to the upper portions of a plant occurs primarily in the xylem and often occurs only in the outermost annual ring (Nobel, 1983), which is driven by water potential gradient.

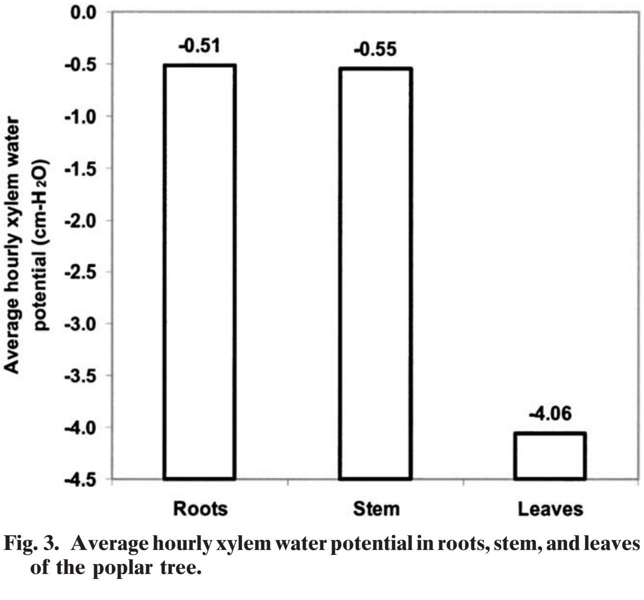

Fig. 3. Average hourly xylem water potential in roots, stem, and leaves of the poplar tree.

Knowledge of xylem water potential is crucial to understand uptake and transport of water, solutes, and carbohydrates in plants. Although this knowledge is difficult to obtain through experimentation, insights can be gained by computer modeling based on mathematical descriptions of the processes involved. Figure 3 shows the average hourly water potentials in the xylem system of the poplar tree. The xylem water potential was high (less negative) in the roots and low (more negative) in the leaves with the stem in between. The water potential head change between the roots and the leaves was 3.55 cm H_2O (i.e., $[-0.55] - [-4.06] = 3.55$), which created a driving force for water flow and chemical transport upward from the roots through the stem to the leaves.

Changes in xylem water potential in roots, stem, and leaves as a function of time during a 96-h simulation period are shown in Fig. 4. This figure shows a daily cycle of xylem water potential decreasing during the day and increasing during the night. In general, the xylem water potential in the roots and stem increased consecutively with time (Fig. 4a and 4b) from about -0.98 and -1.00 cm H_2O at the beginning of the simulation to about -0.19 and -0.20 cm H_2O at 72 h, respectively. That is, the xylem water potential increased 19% in the roots and 20% in the stem within 72 h. This occurs because an equilibrium condition has not yet been reached at such a short time period. An equilibrium condition was approaching after 72 h and continued to 720 h (or 30 d, data not shown). It should be noted that soil water content is an important factor for xylem water

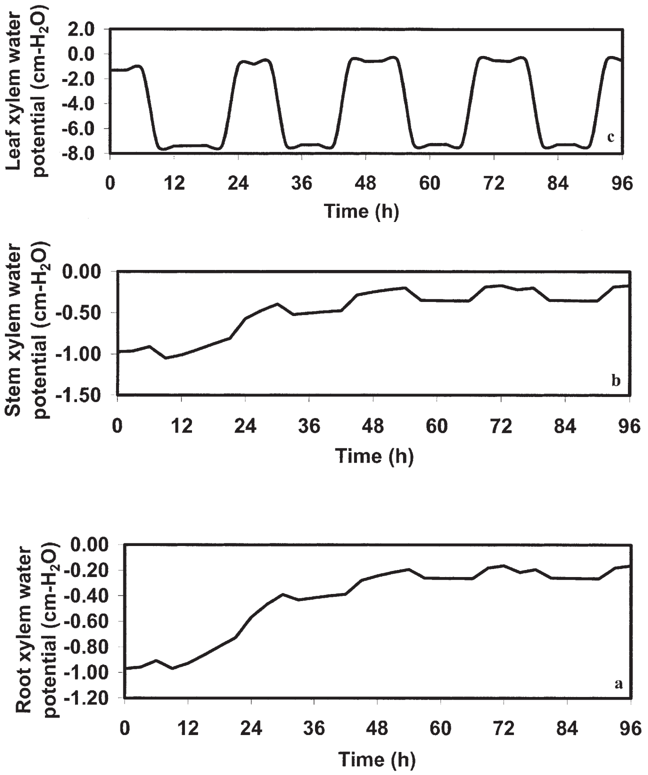

Fig. 4. Simulated xylem water potentials in (a) roots, (b) stem, and (c) leaves as a function of time.

potential variations. Since the soil water content was kept constant through water irrigation (Table 1) in this study, its effect on xylem water potential is trivial.

Changes in xylem water potential in leaves also show a typical pattern: a rapid decrease during the day and a sharp increase at night (Fig. 4c). The difference in xylem water potential between the day and the night at the third day is about 6.00 cm H_2O. During the day, the stomata opened and transpiration removed water from the leaves, thereby decreasing the xylem water potential. At night, the stomata closed and transpiration essentially ceased, thereby increasing the xylem water potential. An equilibrium condition was obtained after 72 h.

Root Uptake of Water and TNT

Figure 5 shows the average daily root water uptake rate and soil TNT concentration depletion as a function of time during the 720-h (or 30-d) simulation period. The root water uptake rate increased rapidly from 0 $cm^3 h^{-1}$ at the beginning of the simulation to about 25 $cm^3 h^{-1}$ in 24 h. This occurred because the initial root xylem water potential was low (-1.0 cm H_2O) and increased 50% (-0.5 cm H_2O) in 24 h (Fig. 4a). Low xylem water potential implies high water suction capacity, thereby increasing root water uptake. After 24 h, the daily average root water uptake rate was constant (Fig. 5). As the root xylem water potential approached an equilibrium condition (Fig. 4a) so did the root water uptake rate.

Depletion of soil solution TNT as a function of time is shown in Fig. 5b. The initial soil TNT concentration was 100 mg L^{-1} and decreased to 10 mg L^{-1} in 14 d. The 90% decrease in soil solution TNT within two weeks occurred mainly as a result of root water uptake.

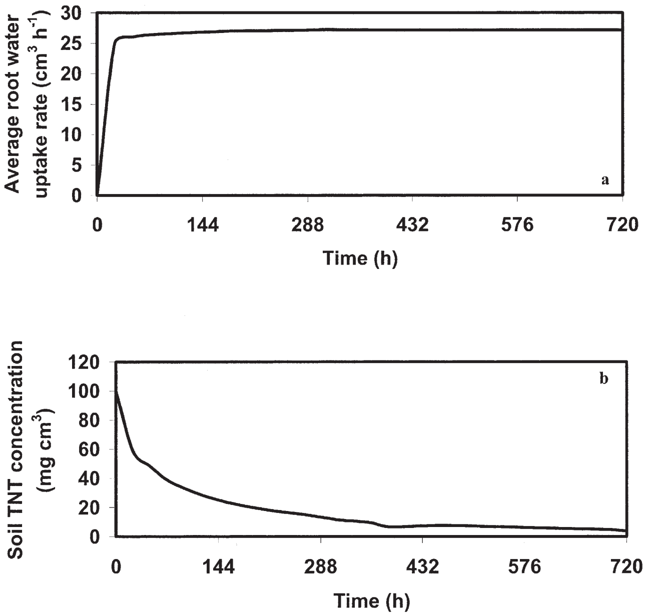

Fig. 5. Simulated (a) root water uptake and (b) soil TNT concentration as a function of time.

No TNT was found in stem and leaf compartments. This simulation finding is consistent with those reported by Mueller et al. (1995), Thompson et al. (1998), and Chang et al. (2004). Changes in TNT mass in the xylem compartments as a function of time are shown in Fig. 6a. The initial TNT concentration in the roots was assumed to be zero. It was found that only about 1% of total TNT mass was in the roots. This finding is similar to that of Mueller et al. (1995). These authors found that most of the radioactivity was present as metabolites and only 0.3 to 1% of the residual radioactivity was found as TNT in roots. A possible explanation of this phenomenon is that most of the TNT uptake by the roots underwent rapid biodegradation and transformed into its daughter products.

Soil TNT Removal and Bioavailability

Depletion of TNT in the soil as a function of time is shown in Fig. 6b. The soil TNT mass decreased with time from 100% initially to 87% at the end of the simulation (30 d). This is equivalent to about 13% of the soil TNT being removed by the poplar tree for the simulation conditions used in this study, resulting mainly from root uptake since TNT is a recalcitrant compound. This finding is somewhat different from the result reported by Thompson et al. (1998) where about 25% of TNT was removed from the soil. We attributed the discrepancy to the differences in initial soil TNT mass used for the two studies. In our study the initial soil solution TNT concentration was 110 mg L^{-1} through the entire soil profile with a depth of 100 cm, whereas in their study the initial soil water TNT concentration was 100 mg L^{-1} with a shorter soil depth of about 20 cm. It should be

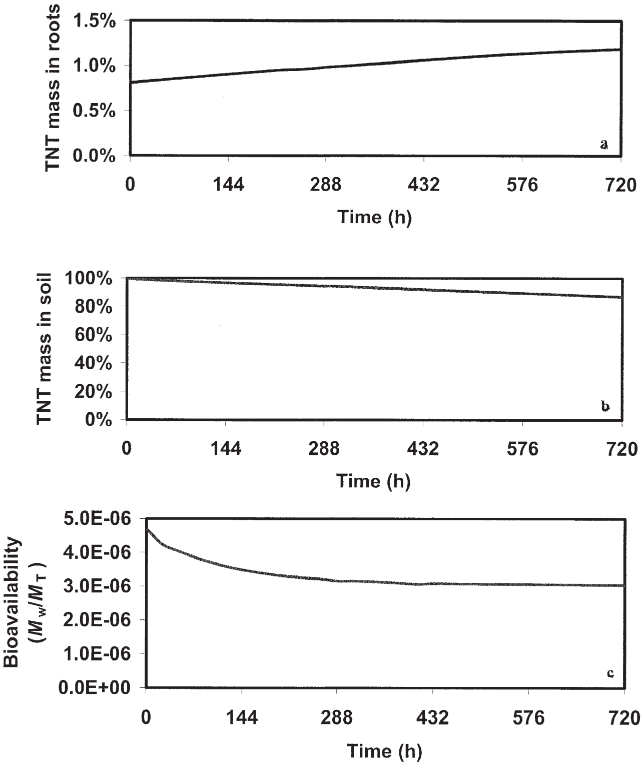

Fig. 6. Simulated TNT mass in (a) roots, (b) soil, and (c) bioavailability as a function of time. Bioavailability is the ratio of the contaminant mass (M_w) in soil solution (which is readily taken up by plants) to the contaminant mass (M_T) in the soil.

pointed out that successful phytoremediation of a contaminated site depends primarily on the bioavailability of the contaminant for plant uptake. However, our finding is similar to that of Sung et al. (2002). These authors reported that about 85% of TNT remained in the soil planted with Johnsongrass [*Sorghum halepense* (L.) Pers.] and Canadian wild rye (*Elymus canadensis* L.) after 30 d.

Sung (2000) defined the bioavailability (B_a) as the ratio of the contaminant mass (M_w) in soil solution (which is readily taken up by plants) to the contaminant mass (M_T) in the soil, that is, $B_a = M_w/M_T$. Figure 6c shows the bioavailability of TNT in the soil as a function of time for a simulation period of 30 d. In general, the soil bioavailability decreased with time due to the depletion of soil solution TNT by the poplar tree. Our simulation further reveals that an equilibrium condition or constant bioavailability (3.1×10^{-6}) was approaching in 14 d. At this bioavailability and time, the soil solution TNT concentration was about 10 mg L^{-1} (Fig. 5b).

REFERENCES

Aitchison, E.W., S.L. Kelley, and J.L. Schnoor. 2000. Phytoremediation of 1,4-dioxane by hybrid poplar trees. Water Environ. Res. 72:313–321.

Arienzo, M. 2000. Degradation of 2,4,6-trinitrotoluene in water and soil slurry utilizing a calcium peroxide compound. Chemosphere 40:331–337.

Boersma, L., F.T. Lindstrom, and S.W. Childs. 1991. Model for steady state coupled transport in xylem and phloem. Agron. J. 83:401–415.

Boersma, L., F.T. Lindstrom, C. McFarlane, and E.L. McCoy. 1988. Uptake of organic chemicals by plants: A theoretical model. Soil Sci. 146:403–417.

Chang, Y.Y., Y.S. Kwon, S.Y. Kim, I.S. Lee, and B. Bae. 2004. Enhanced degradation of 2,4,6-trinitrotoluene (TNT) in a soil column planted with Indian mallow (Abutilon avicennae). J. Biosci. Bioeng. 97:99–103.

Hillel, D. 1982. Introduction to soil physics. Academic Press, New York.

Hughes, J.B., J. Shanks, M. Vanderford, J. Lauritzen, and R. Bhadra. 1997. Transformation of TNT by aquatic plants and plant tissue cultures. Environ. Sci. Technol. 31:266–271.

Jarvis, A.S., V.A. McFarland, and M.E. Honeycutt. 1998. Assessment of the effectiveness of composting for the reduction of toxicity and mutagenicity of explosive-contaminated soil. Ecotoxicol. Environ. Saf. 39:131–135.

Kaplan, D.L. 1990. Biotransformation pathways of hazardous energetic organonitro compounds. p. 155–182. *In* A. Chakrabarty and G.S. Omenn (ed.) Advances in applied biotechnology. Vol. 4. Biotechnology and biodegradation. Portfolio, Houston, TX.

Lindstrom, F.T., L. Boersma, and S. Yingjajaval. 1990. CTSPAC: Mathematical model for coupled transport of water, solutes, and heat in the soil-plant-atmosphere continuum. Volume 1. Mathematical theory and transport concepts. Bull. 676. Agric. Exp. Stn., Oregon State Univ., Corvallis.

Mueller, W.F., G.W. Bedell, S. Shojaee, and P.J. Jackson. 1995. Bioremediation of TNT wastes by higher plants. p. 222–230. *In* Proc. of the 10th Annual Conf. on Hazardous Waste Res., Manhattan, KS. 23–24 May 1995. Kansas State Univ., Manhattan. Also available online at www.engg.ksu.edu/HSRC/95Proceed/mueller.pdf (verified 7 Apr. 2005).

Nedunuri, K., V. Govindaraju, and R.S. Chen. 2000. Evaluation of phytoremediation for field-scale degradation of total petroleum hydrocarbons. J. Environ. Eng. 126:483–490.

Nobel, P.S. 1983. Biophysical plant physiology and ecology. Freeman and Company, San Francisco.

Ouyang, Y. 2002. Phytoremediation: Modeling plant uptake and contaminant transport in the soil-plant-atmosphere continuum. J. Hydrol. (Amsterdam) 266:66–82.

Pivetz, B.C. 2001. Phytoremediation of contaminated soil and ground water at hazardous waste sites. EPA/540/S-01/500. USEPA, Ada, OK.

Schackmann, A., and R. Muller. 1991. Reduction of nitroaromatic compounds by different Pseudomonas species under aerobic conditions. Appl. Microbiol. Biotechnol. 34:809–813.

Schnoor, J.L., L.A. Licht, S.C. McCutcheon, N.L. Wolfe, and L.H. Carreira. 1995. Phytoremediation of organic and nutrient contaminants. Environ. Sci. Technol. 29:318A–323A.

Sung, K. 2000. Phytoremediation and bioremediation of hydrocarbons: Modeling and field application. Ph.D. diss. Texas A&M Univ., College Station.

Sung, K., C.L. Muster, R. Rhykerd, M.C. Drew, and M.Y. Corapcioglu. 2002. The use of box lysimeters with freshly contaminated soils to study the phytoremediation of recalcitrant organic contaminants. Environ. Sci. Technol. 36:2249–2255.

Thompson, P.L., L.A. Ramer, and J.L. Schnoor. 1998. Uptake and transformation of TNT by hybrid poplar trees. Environ. Sci. Technol. 32:975–980.

Trapp, S., and U. Karlson. 2001. Aspects of phytoremediation of organic pollutants. J. Soils Sediments 1:37–43.

Voudrias, E.A., and K.S. Assaf. 1996. Theoretical evaluation of dissolution and biochemical reduction of TNT for phytoremediation of contaminated sediments. J. Contam. Hydrol. 23:245–261.